CHAPTER 5

RESULT AND DISCUSSION

5.1 Introduction

In this chapter, the experimental data generated using the fabricated drilling setup have been tabulated, for analysis and discussion on the findings. The results have been presented graphically also, whenever possible, for better understanding of the influence of various parameters. For minimizing the errors (whether measurement error or machine error) each operation has been repeated five times under identical conditions, and the average value of the parameter has been taken into consideration. The data presentation and analysis for various performance parameters to achieve the goal of this study, have been discussed below.

5.2 Flushing Rate Optimisation

The variation in fluid flow speed was obtained by the flow adjuster (marked 'P' in Fig. 3.2), to identify the optimum flushing rate, while keeping 450 RPM and 29.02 N and

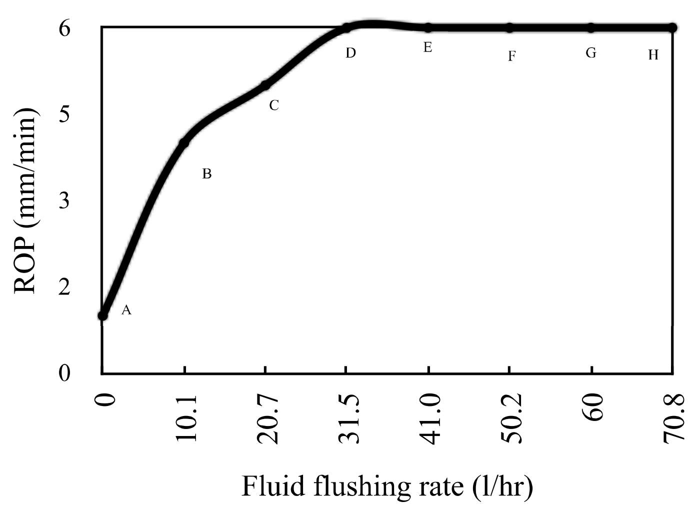

Fig. 5.1: Optimisation of Flushing Rate

water (drilling fluid) as constant parameter. The data collected have been presented in Fig. 5.1, having fluid flushing rate on X-axis and ROP on Y-axis. While drilling, in the absence of flushing fluid, the bit can drill only upto to a limited depth. If drilling is still continued, it either gets stuck or energy is simply wasted in regrinding of the drill cuttings – without any further penetration. This situation is presented as 'A' in Fig. 5.1.

At the micro-level, the pre-existing and newly developed fractures may be filled with fine drill cuttings (generated by regrinding) and block the interaction of bit and fresh rock surface. At points 'B', 'C' and 'D', an increment in ROP has been observed with the increment in flushing rate compared to the ROP at point A. With an increment in flushing rate by 31.5 L/hr, 500% increment in ROP has been observed, while comparing the points 'A' and 'D'. These results may be due to the continuous improvement in hole cleaning efficiency by the increment in the amount of fluid utilized in the removal of drill cuttings and drill fines from the hole and the micro-fractures respectively. And after point 'D' (i.e. E, F, and G), despite the increment in flushing rate, no considerable increment in ROP was observed, Also, an excessive amount of fluid was overflowing.

As it is adduced by the results of this experiment that flushing rate lower than the optimum, might lead to thickening of mud, and improper cleaning of the bit-rock interface - thus, resulting in a poor drilling rate, bit jam, over heating, etc. On the other hand, very high flushing rate would lead to unnecessary wastage of the flushing fluid and pilferage of energy that made the optimization of drilling fluid more crucial. So, the point 'D' shows the optimum performance at optimum fluid flushing rate of 31.5 l/hr.

5.3 Effect of Holes Position on Rate of Penetration (ROP)

For this project work, cuboid shaped rock (fine grain sandstone) samples were prepared having maximum permissible dimensions 40 cm (L) X 23 cm (W) X 23 cm (H), as shown in Fig. 5.2. The distance of a hole (to be drilled) from the free face or adjacent hole directly affects the rate of penetration (ROP). So, it is necessary to identify the suitable positions on the rock sample to drill the holes. The positions should be decided so that there is no influence of the adjacent holes on the penetration rate and energy consumption in drilling.

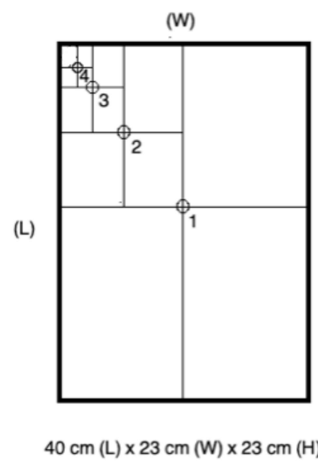

Fig. 5.2: Pre-defined Location of Holes

For aforesaid purpose, keeping the other parameters constant (450 RPM, 36.09 N, water as drilling fluid and 3 min drilling time), the working surface of a sample (L X W) was initially divided into quarters by imaginary lines, and the first hole was drilled at the intersection of lines (tagged as '1' in Fig. 5.2). Afterward, the individual quarters were sub-divided in to four equal parts and holes was drilled on the centre of it, as tagged '2' in Fig. 5.2. Following the same process, hole no. 3, and hole no. 4 were drilled (as shown in Figure 5.2). The hole no. 4 was drilled at the edge of rock sample and at the very less partition thickness or the spacing of 0.7 cm from hole no. 3, depending on the size of sample and diameter of bit. The same procedure was performed with 5 different samples and to show the manner of data collection, the results produced from a sample are presented in Table 5.1. On the basis of experimental data, it could be concluded that, there is no considerable variation in penetration rate and energy consumption due to different positions of hole, while drilling upto the hole partition of 0.7 cm.

Table 5.1: Effect of hole position on sample

Sample No.	Hole no.	Penetration Rate (mm/min)	Energy (kWh)
1 to 5	1	8.12	3.970
-	2	8.22	3.948
-	3	8.18	3.880
-	4	8.25	3.937

It may be due to several reasons, such as the higher confinement of fine-grain sandstone rock, higher mechanical strength of rock like compressive, and shear, and minimum discontinuities in the sample, which provides the high resistivity deformation. Also, the rotary drilling operation by impregnated core diamond bit with flushing fluid may imply minimum shock to both the rock sample and the bit, which causes smooth operation. So, the optimum distance between adjacent holes was kept 1 cm by having factor of safety (FOS) 30%.

5.4 Constant Energy Consumption (CEC)

The process and importance of constant energy consumption is discussed in sub-chapter 4.4.2. To calculate the same, 11 variations of RPM have been applied, and energy readings have been recorded with real-time measurement setup. While there is no contact between bit and rock, the input power is consumed by the various machine parts (motor, pump, machine internal friction, all measuring meters and machine internal circuit),. An example of data collection for CEC is given in Table 5.2.

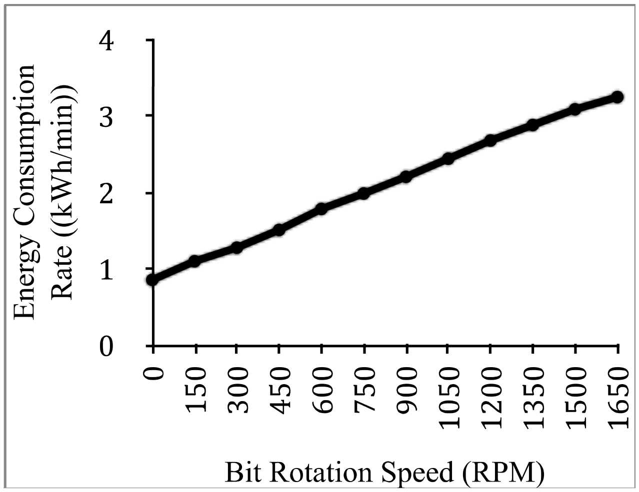

Fig. 5.3: Constant Energy Consumption at no Load

Table 5.2: Data collection Sheet for CEC Calculation

Bit Rotation Speed (RPM)	Time in video (min)	Energy (kWh)	Energy Difference (kWh)	Average Energy consumption
1300	1:26	27.718	—	0.050 kWh/s or 3.000 kWh/min
	1:27	27.762	0.044	
	1:28	27.818	0.056	
	1:29	27.863	0.045	
	1:30	27.918	0.055	

And, average values of CEC at each RPM is given in Table 5.3. These average values were used in further calculation for energy consumption in drilling process, and also for specific energy consumption (SEC). For each RPM, the energy readings were recorded for 5 min and average was taken. Also, a constant increment in energy consumption rate is noticed in Figure 5.3, with the raise in bit rotational speed.

The calculation procedure for the measurement of specific energy consumption (SEC) in drilling is shown through an example: Say, a hole is drilled at 300 RPM with 36.09 N load on bit for 30 s. The data collected for aforesaid condition is presented in Table 5.4. Now, for 300 RPM constant energy consumption (E_{300}) is 0.0212 kWh/s, from Table 5.3.

Table 5.3: Constant Energy Consumption at no Load

Sr.	Bit Rotation Speed (RPM)	Energy Consumption Rate	
		Per second (kWh/s)	Per minute (kWh/min)
1	150	0.0183	1.099
2	300	0.0 212	1.277
3	450	0.0251	1.509
4	600	0.0297	1.783
5	750	0.0330	1.985
6	900	0.0367	2.203
7	1050	0.0406	2.440
8	1200	0.0446	2.678
9	1350	0.0480	2.881
10	1500	0.0514	3.086
11	1650	0.0541	3.246

Table 5.4: Data Sheet for SEC Calculation

<table>
<tr><th>Bit Rotational speed (RPM)</th><th>Load on bit (N)</th><th>Time in video (s)</th><th>Time in drilling (s)</th><th>Depth of hole (mm)</th><th>Energy Reading (kWh)</th><th>Total Energy consumption in operation (Final-Initial) (KWh)</th></tr>
<tr><td rowspan="2">300</td><td rowspan="2">36.09 N</td><td>118 (Start)</td><td rowspan="2">30</td><td rowspan="2">3</td><td>2.099 (Initial)</td><td rowspan="2">2.903-2.099 =0.804</td></tr>
<tr><td>148 (End)</td><td>2.903 (Final)</td></tr>
</table>

So, Energy consumption by drilling (ED)

= [Total Energy consumption in operation (ET)]

— [Constant Energy at 300 RPM X Time in Drilling (t)]

= 0.804 — (0.0212 X 30)

= 0.168 kWh

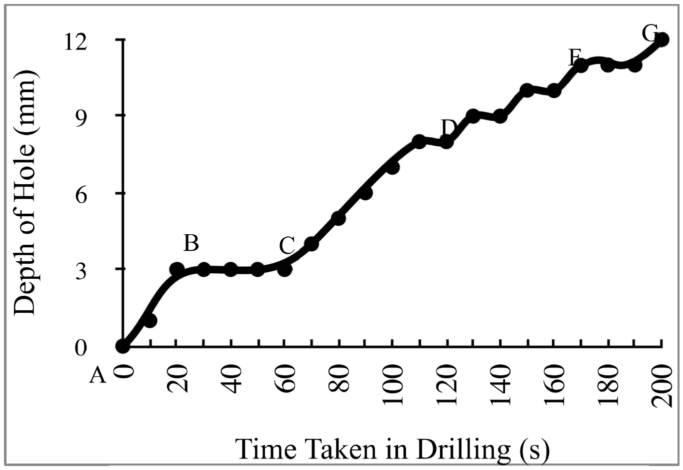

Fig. 5.4: Impact of flushing media on ROP

Using Eq. (4.2), Specific Energy consumption (SEC) = 0.168 / (170.345 x 3)

= 32.874 X 10^{-5} kWh/mm^3

5.5 Impact of Flushing Fluid

To investigate the role of flushing fluid, the operation was started without any flushing media under 750 RPM and 36.09 N load on bit. Thereafter, tap water was introduced in the drilling operation, when no further progress was observed in the depth of hole. The optimum flushing rate of drilling fluid i.e. 31.5 L/hr (as obtained from Fig. 5.1) was implemented in this investigation and results are presented in Fig 5.4. It is adduced from Figure 5.4, that from point ‘A’ to point ‘B’, rapid increment in the depth is observed for a short depth of about 3 mm. For better presentation, the gradient of curve has been calculated between various points by considering 1 mm depth and 10 s time interval as unit and the results have been shown in Table 5.5. The gradient between points ‘A’ and ‘B’ in Fig. 5.4 was 1.0 (as shown in Table 5.5), which may be due to the shock loading at the bit-rock interface, at initial interaction. From point ‘B’ to point ‘C’ it is observed that, the gradient of curve was ‘0 (Zero)’, due to the absence of flushing fluid. At this condition, only regrinding of drill cuttings took place. The fines developed by regrinding may enter in the fractures at bit-rock interface, and resulted in reduction in drilling rate. At the extreme situation, when the accumulation of re-grinded drill cuttings in the hole exceeds, no further penetration could be achieved.

After that, from point ‘C’ to point ‘D’, as water has been introduced as flushing fluid, an appreciable increment was observed in the depth (with curve gradient 0.86, as shown in Table 5.5). Due to the cleaning of drill cuttings from the bit-rock interface and fractures by fluid, fresh surface was exposed to the bit tip which lead to the increment in ROP. It may also be due to the reduction in the friction between the surfaces of a fracture [Yan et al. 2018] **,** due to the lubrication properties of drilling fluid. It resulted in the weakening of a fracture, that led towards the increment in ROP.

Table 5.5: Gradient Calculation for Slope of Curve in fig.5.4

Sr.	**From Point**	**To Point**	**Gradient** [Units on X axis(1mm) / Units on Y axis (10 s)]	**Gradient**
1	A	B	3/3	1.0
2	B	C	0/4	0
3	C	D	6/7	0.86
4	D	G	3/7	0.43

5.6 Effect of Depth of the Hole on ROP

From Figure 5.4, it is apparent that from point ‘C’ to ‘D’, bit had drilled 6 mm depth in 70 s (with curve gradient 0.085), whereas after point ‘D’, in the same time interval, bit had achieved 3 mm depth in the rock (with curve gradient 0.43). The gradient of curve between point ‘D’ to ‘G’ was approximately half of the gradient from ‘C’ to ‘D’, as shown in Fig. 5.4 and Table 5.5. As the bit penetrates deeper in the rock, after point ‘D’, the drag between surrounding walls and drill rod got increased, and led to a considerable reduction in the rate of penetration. It can also observed from the slope of the graph from point C to D and D to G in Figure 5.4.

At points ‘B’, ‘C’ and ‘D’, an increment in ROP has been observed with the increment in flushing rate respectively. These results may be due to the continuous improvement in hole cleaning efficiency by the increment in the amount of fluid utilised in removal of drill cuttings.And after point ‘D’ (i.e. E, F, and G), despite the increment in flushing rate, no considerable increment in ROP was observed and also an excessive amount of fluid was overflowing.

5.7 Effect of Machine Parameters on Drilling Performance

The data sheet used to collect the experimental data and present the performance parameters, is given in Table 5.6. The constant parameters for this experiment were as follows:

- Rock type (sandstone),
- Bit type (impregnated diamond core bit),
- Bit dia. (19/12 mm),
- Flushing rate (31.5 l/hr), and
- Base drilling fluid (tap water)

The variables are bit rotational speed (RPM), load on bit (N), type & concentration of drilling fluid additives. They were varied in the range of :

- Bit rotational speed (RPM): 150 to 1650 RPM
- Load on bit (N) : 26.28 N to 85.12 N
- Type of polymers: natural polymer - 4 nos., laboratory synthesised - 5 nos.
- Concentration of drilling fluid additives: 10 ppm to 110 ppm

In Table 5.6, column 12 to 16 are the performance parameters including bit temperature, machine vibration, and bit wearing calculated with help of data collected by experimentation (as presented in column 1 to 11). The bit temperature, and machine vibration, were also measured as performance parameters. The effect of various machine parameters on performance parameters are discussed here for all the variations applied.

5.7.1 Effect of Bit Rotational Speed and Load on Bit

While keeping rock type (sandstone), bit type (impregnated diamond core bit), bit dia. (19/12 mm), flushing rate (31.5 l/hr), and drilling fluid (tap water), drilling time (3 min) as constant parameters, their effect on ROP, energy, SEC, bit temperature, RRR and drill spindle vibration have been presented in graphical format and discussed here.

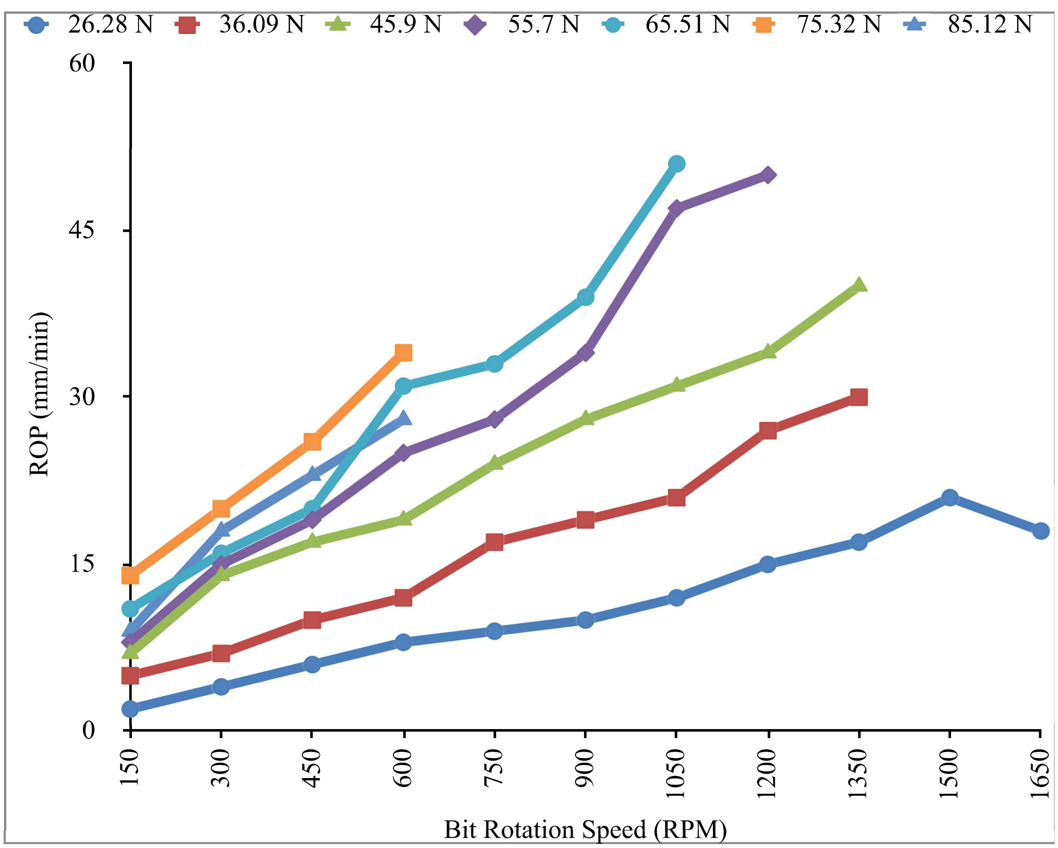

Fig. 5.5:Effect on ROP achieved in drilling for 1 min.

5.7.1.1 Effect on ROP

The bit rotational speed has been varied from 150 to 1650 RPM, to apply 11 variations at equal interval of 150 RPM. For better understanding, the effect of RPM and load on bit variations on ROP was measured and presented for 1 min and 3 min drilling separately in Figure 5.5 and 5.6 respectively.

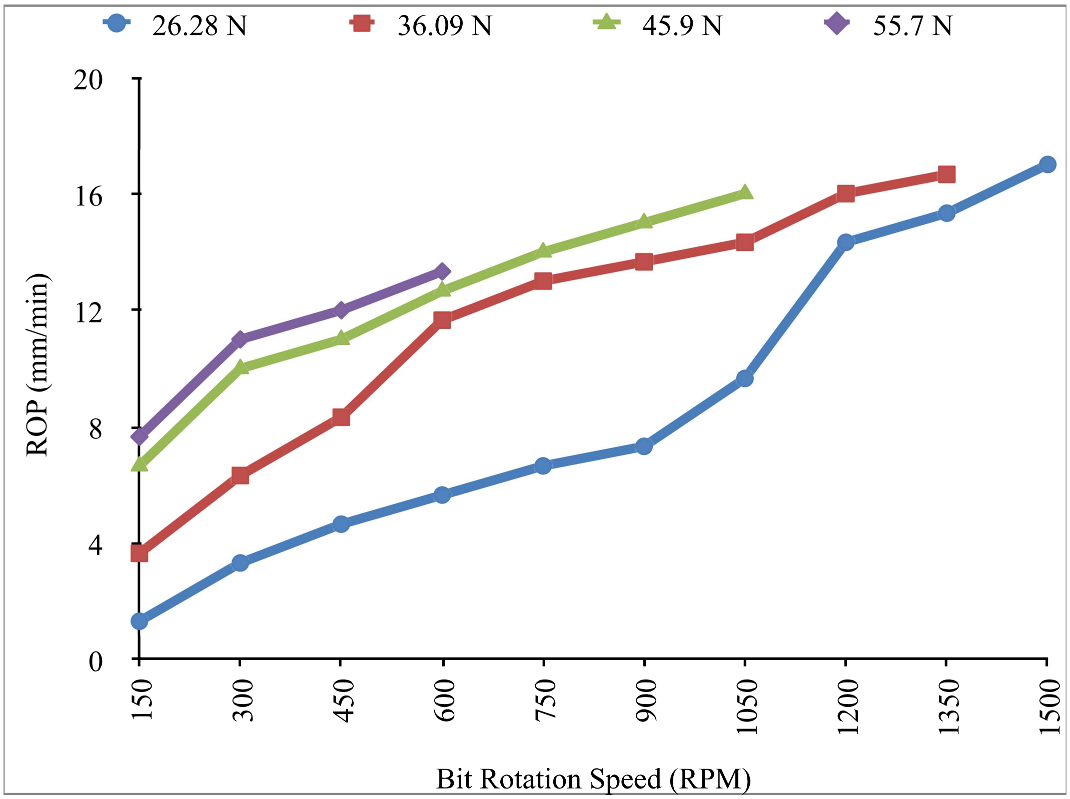

Fig. 5.6: Effect on ROP achieved in drilling for 3 min.

Observations

From the Fig. 5.5, it was observed that for 1 min drilling duration, the ROP was increased with the RPM load on bit. It was found dependent on the machine's capability to maintaining the constant RPM with the help of RPM feed-back system. At 26.28 N load on bit with 1650 RPM rotational speed, a drop in ROP was noticed. It was due to the limitations of the motor, the setup was unable to maintain the constant RPM throughout the operation. And with 3 min drilling duration, it was observed that for the load on bit higher than 55.7 N, either the bit got stuck in rock or the bit achieved the full depth of hole prior to 3 min drilling interval. Also a significant reduction in ROP was noticed with the increment in duration of drilling from 1 min to 3 min.

5.7.1.2 Effect on Energy Consumption

The energy consumption in drilling operation has been studied with a predefined wide range of variation in bit rotational speed and load on bit. The results have been presented for the 1-min drilling duration and 3-min drilling duration separately in Figures 5.7 and 5.8 respectively.

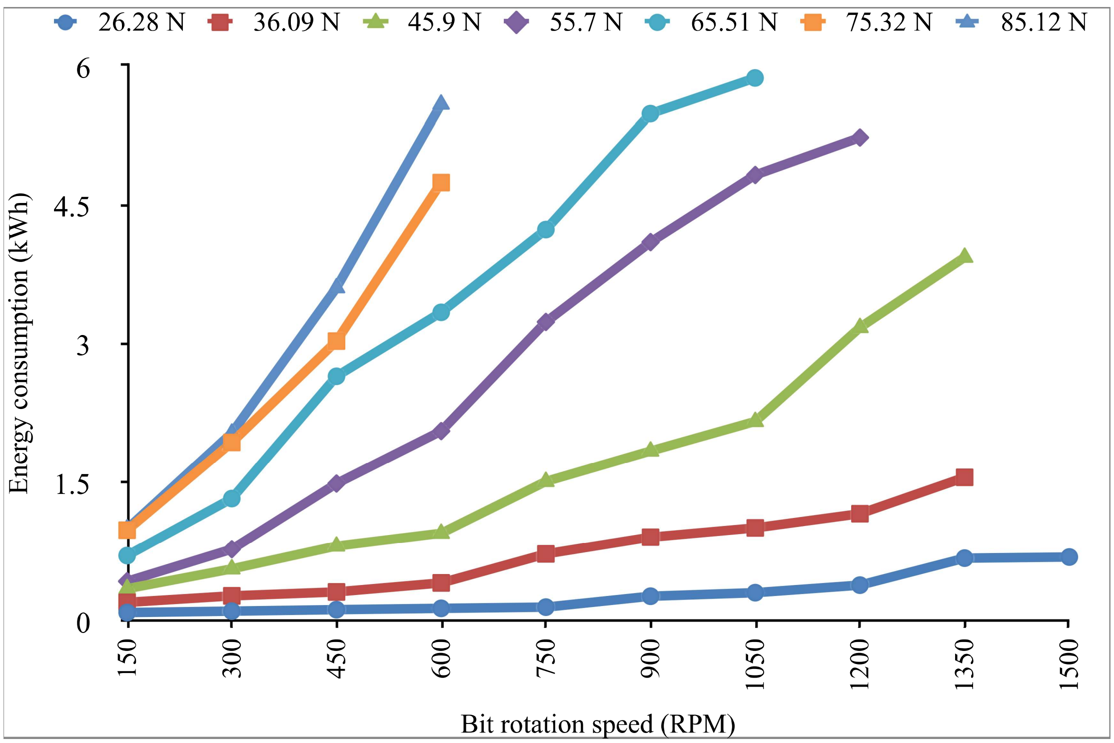

Fig. 5.7: Effect on energy consumption in drilling for 1 min.

Observations

From the Figs 5.7 & 5.8, it was observed that for both the drilling durations i.e. 1 min and 3 min, the energy consumption increased with the RPM increment for all the 7 variations of load on the bit.

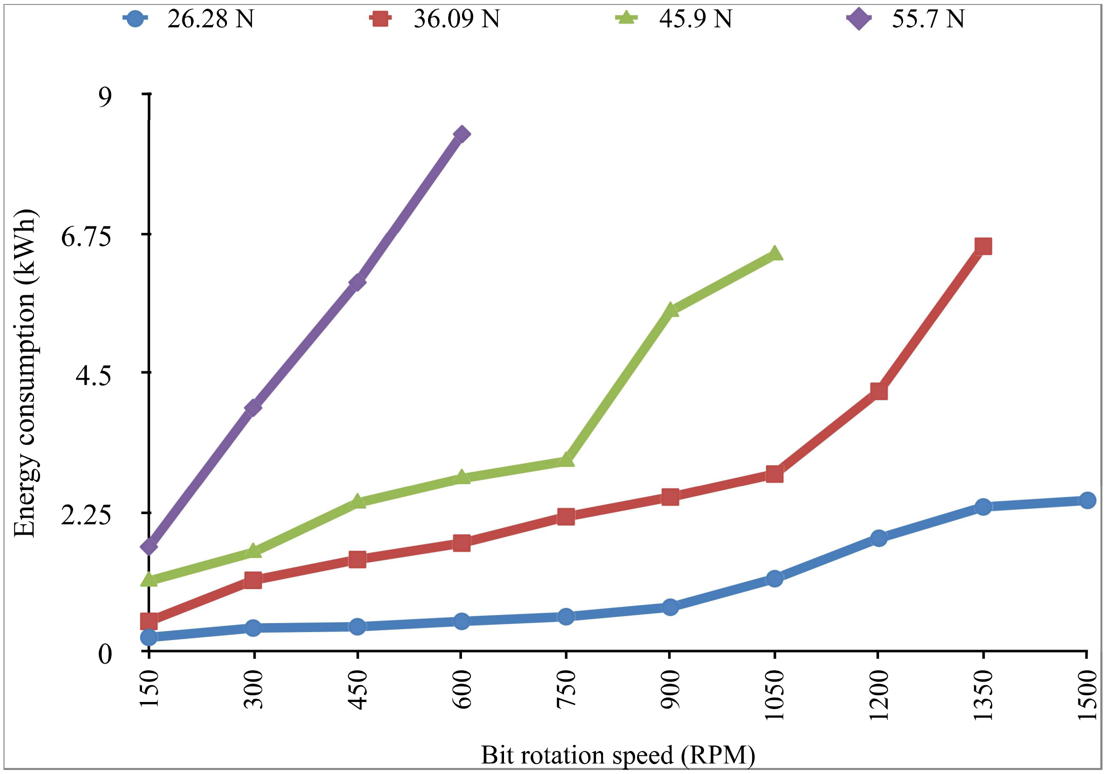

Fig. 5.8: Effect on avg. energy consumption of drilling for 3 min.

5.7.1.3 Effect on Specific Energy Consumption (SEC)

The variations in SEC for the predefined combination of machine parameters are presented in Figures 5.9 & 5.10 for the 1-min drilling duration and 3-min drilling duration respectively.

Observations

The SEC bears the combined effects of ROP and energy consumption in drilling. It was observed from both the Figs. 5.9 and 5.10, that for the low loads on bit (i.e. 2.68 N, 36.09 N and 45.9 N), the SEC was very low for all the applied RPM. Afterwards, for higher loads (above 55.7 N), high fluctuations in SEC was observed.

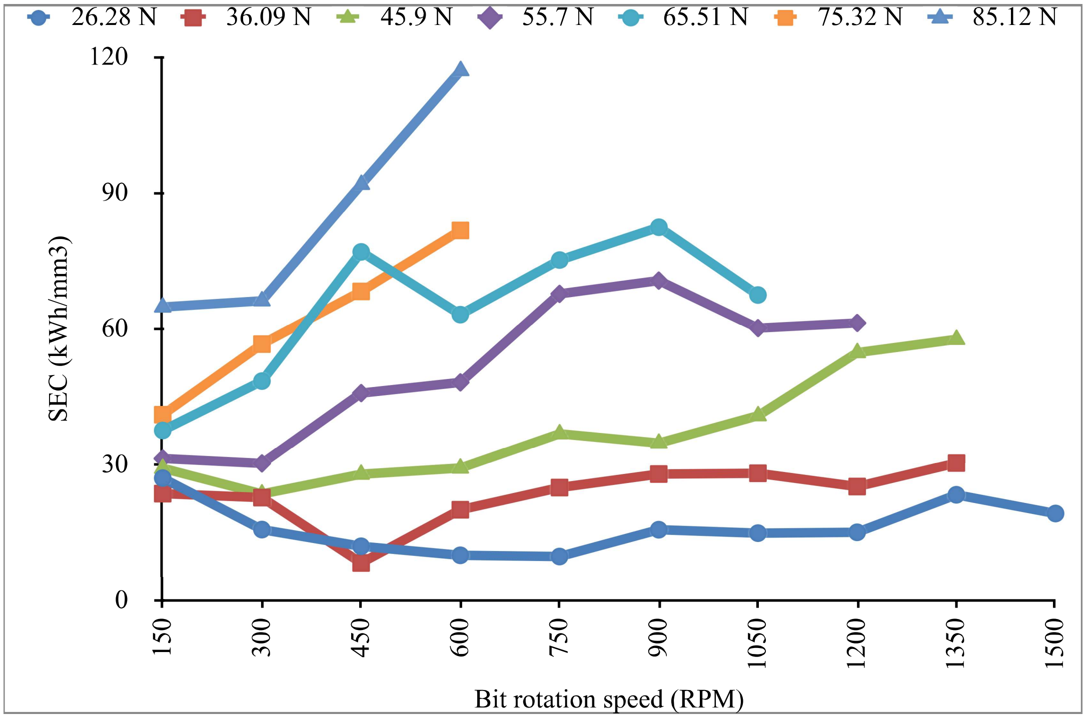

Fig. 5.9: Effect on SEC in drilling for 1 min

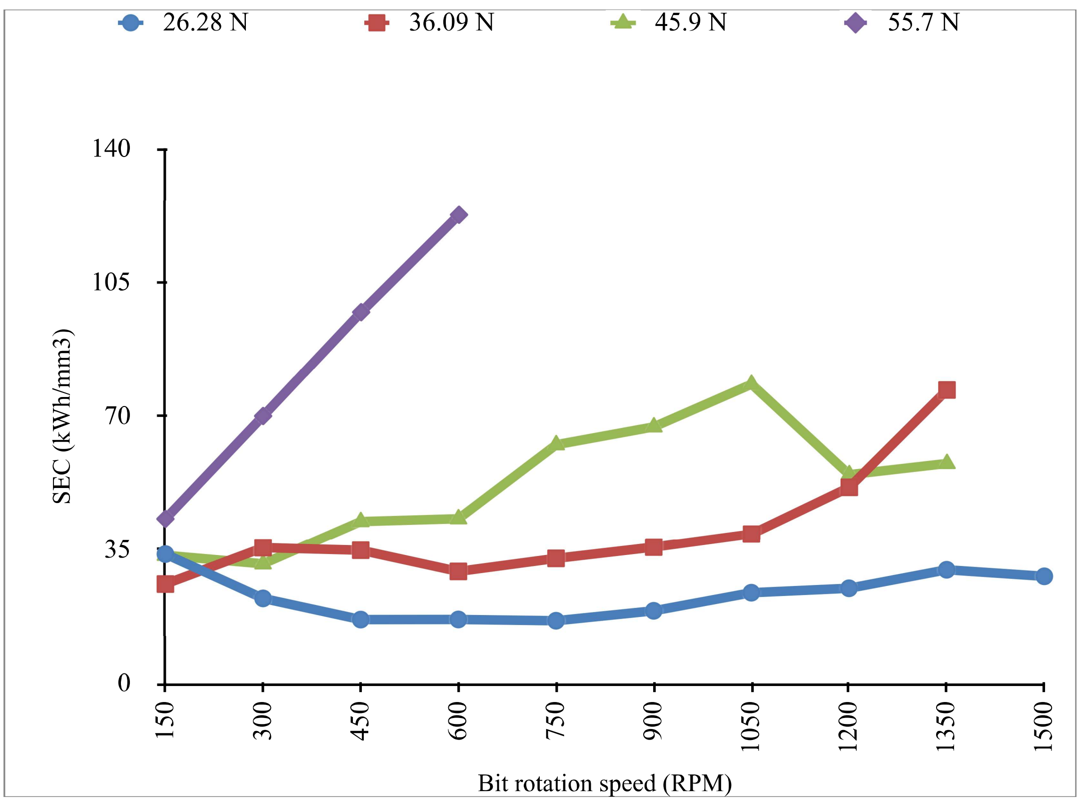

Fig. 5.10: Effect on avg. SEC of drilling for 3 min

5.7.1.4 Effect on Rock Removal Rate (RRR)

The variations in RRR for predefined combination of machine parameters are presented in Figures 5.11 and 5.12 for the 1-min and 3-min drilling duration respectively. The RRR has combined effects of ROP and cross-section of the hole .

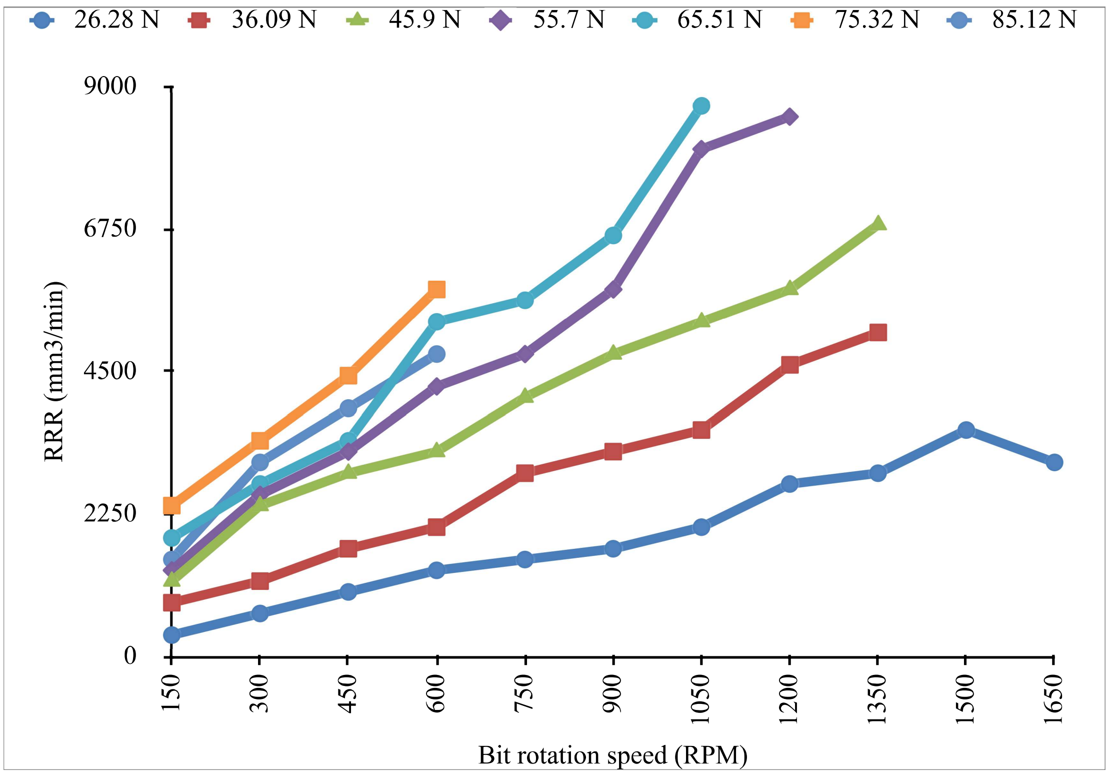

Fig. 5.11: Effect on RRR achieved in drilling for 1 min.

Observations

From the Figs. 5.11 and 5.12, it was observed that the RRR increased with the RPM increment at all the variations of the applied load on the bit. But, for 26.28 N load on bit with 1650 RPM, a sudden rise in RRR was noticed. This was due to the drop in ROP as shown in Fig. 5.5. The value of RRR depends on the ROP, bit type and bit diameter.

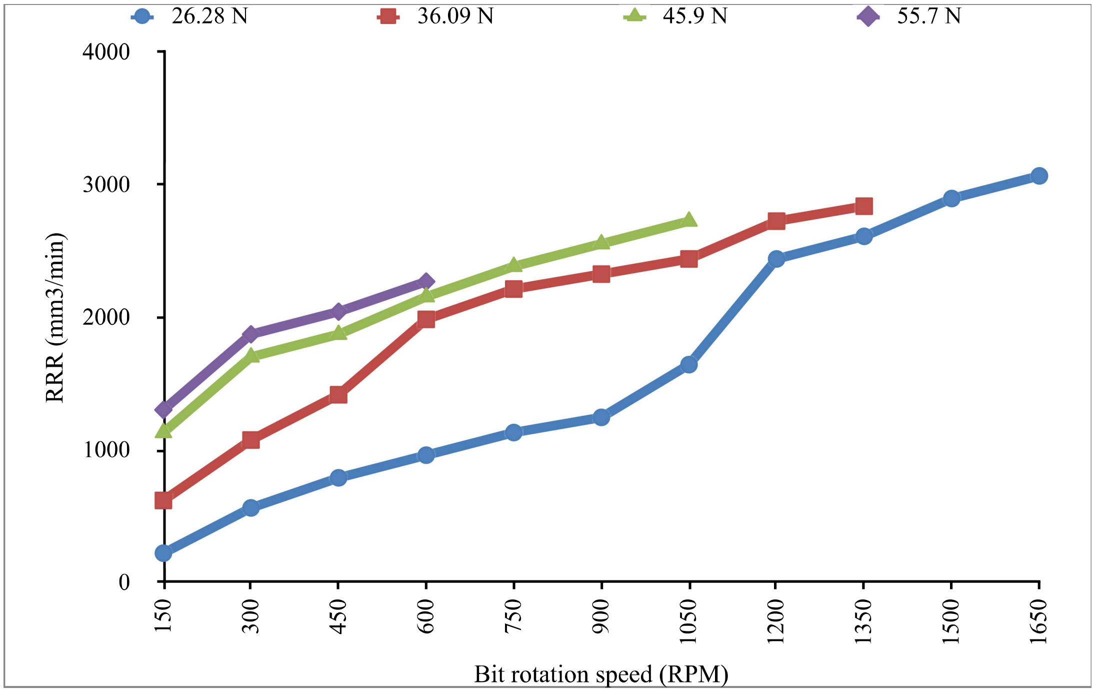

Fig. 5.12: Effect on avg. RRR of drilling for 3 min.

5.7.1.5 Effect on Bit Temperature

During the bit & rock interaction, the cutting tip of the bit gets heated up due to the frictional acting on it. The effects of rotational speed and load on the bit, temperature of the bit was measured and presented in Fig. 5.13.

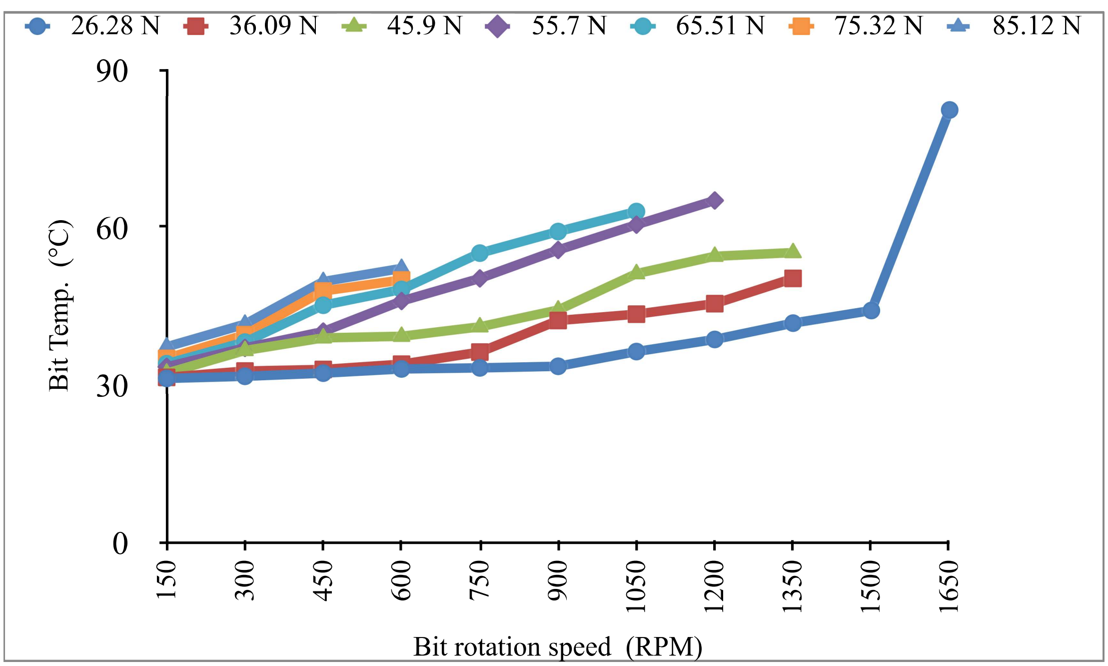

Fig. 5.13: Effect on bit temperature after drilling for 3 mins.

Observations

From the Fig 5.13, it was observed that the bit temperature increased with the RPM increment for all the variations of load applied on the bit. At 26.28 N load on bit with 1650 RPM bit rotational speed, a sudden rise in ROP was noticed. It may be due to regrinding of drill cuttings at high RPM of bit, which causes rise in bit temperature. Also for the aforesaid combination, there was a drop in ROP. (Fig. 5.5).

5.7.1.6 Effect on Drill Spindle Vibration

The vibration rate of drill spindle has been studied to identify the effect of various parameters like, effect of bit RPM without drilling and with drilling, effect of load on the bit, and effect of rate of penetration (ROP) on vibration. The results of this study are presented through Fig. 5.14, 5.15, 5.16 & 5.17. The vibration values were measured in root mean square (RMS) of X, Y and Z direction and vibration total value (VTV).

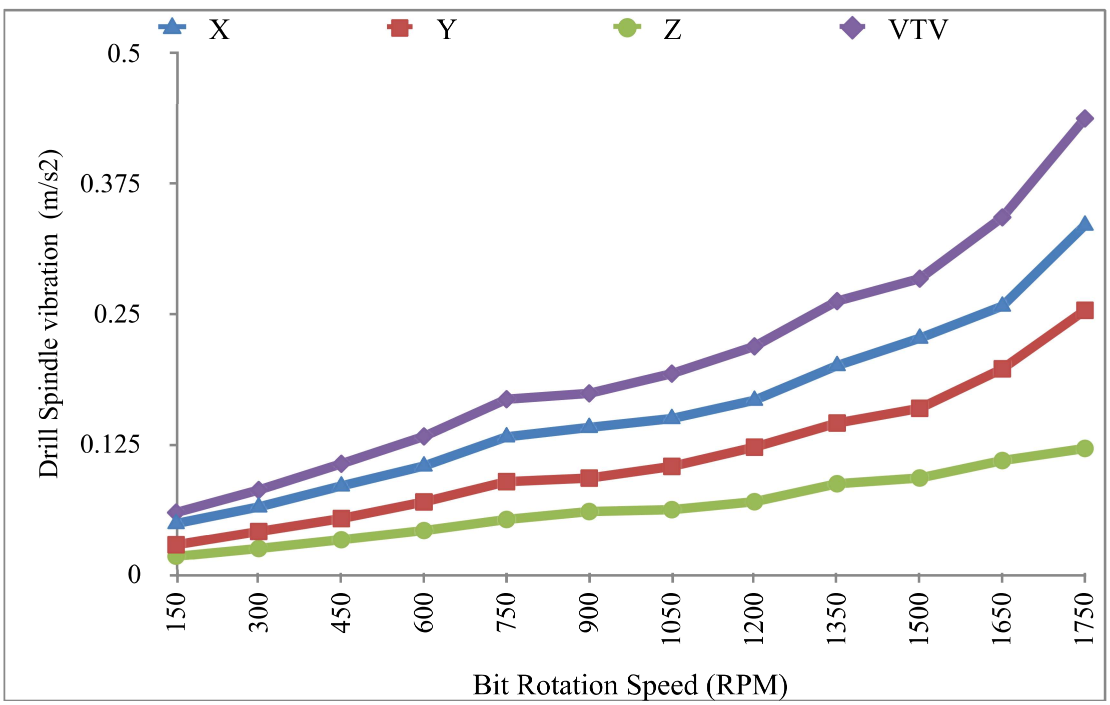

Fig. 5.14: Effect of RPM variation on drill spindle vibration without drilling

Observations

From the Figs 5.14 & 5.15, it was observed that the spindle vibration increased with the RPM raise, for both the conditions, i.e. with and without drilling operation. On the other hand, with the raise in load on bit, the vibration decreased for all the applied loads (as shown in Fig. 5.16). It was also noticed that the vibration of spindle also increased with the increase in ROP (as shown in Fig. 5.17).

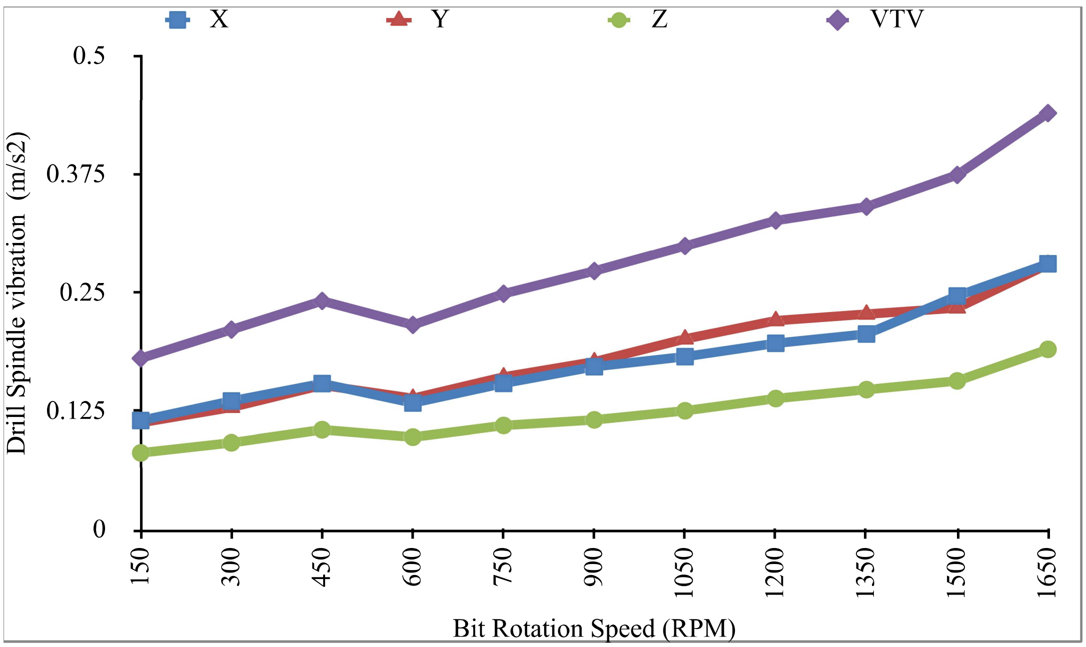

Fig. 5.15: Effect of RPM variation on drill spindle vibration with 26.28 N load on bit and water as drilling fluid

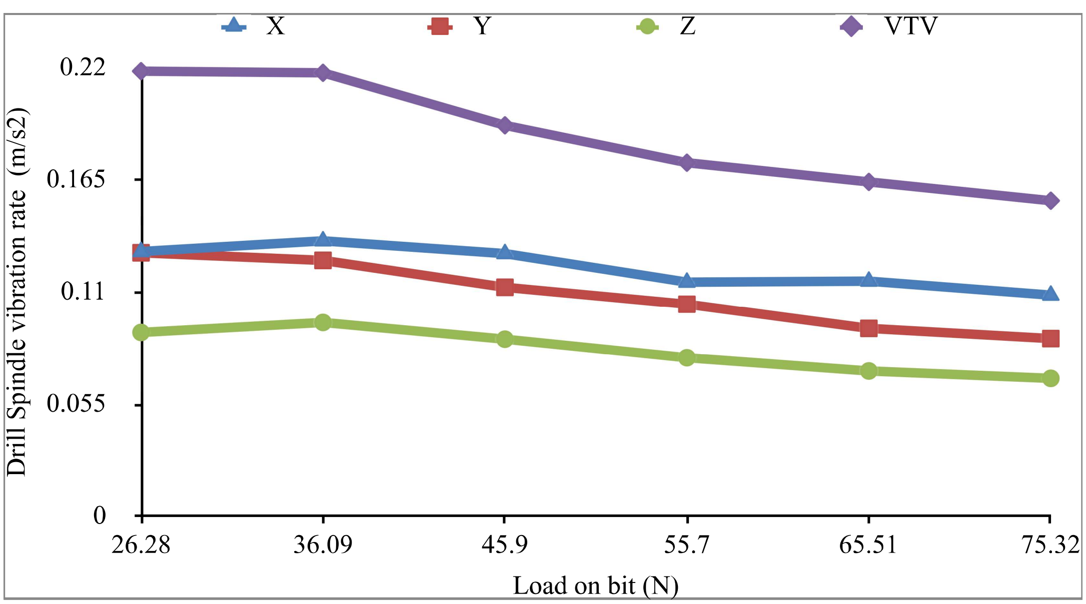

Fig. 5.16: Effect of Load on bit variation on drill spindle vibration with 600 RPM and water as drilling fluid and water as drilling fluid

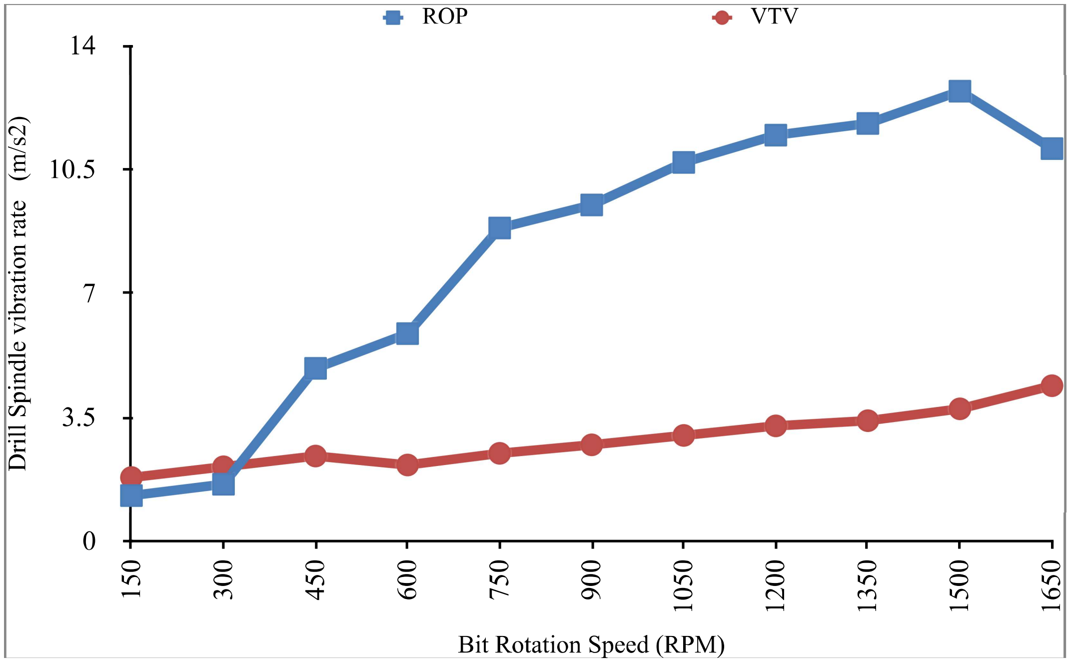

Fig. 5.17: Effect of ROP on drill spindle vibration with 26.28 N load on bit and water as drilling fluid

5.7.2 Effect of Drilling Fluids

In this experiment the rock type (sandstone), bit type (impregnated diamond core bit), bit dia. (19/12 mm), bit speed (750 RPM), load on bit (45.9 N), and flushing rate (31.5 l/hr), were kept as constant parameters. And the effect of various concentrations (10 , 30 , 50 , 70 , 90 , 110 and 130 ppm) of fluid additives to tab water i.e. CMC, PAM, GG, PAMPS, St-g-PAM, ST-g-PAMPS, AP-g-PAM, Hy-St-g-PAM, Hy-AP-g-PAM has been compared with performance parameters of tap water alone. The experimental results on the effect of various concentrations of additives on drilling performance parameters have been discussed here. The salient findings have been presented graphically. It was observed from the previous results (Fig. 5.5 to 5.17), that with the increment in the bit rotation speed (RPM) and load on bit (N), high fluctuations in performance parameters were noticed. It lead to the opting of a combination of machine parameters having significant as well as stable performance, for further experiments. A data sheet was used to collect the experimental data and present the performance parameters (Table 5.7). In this table, column no. 1 to 13 give the experimentally collected data, and columns 14 to 19 give the calculated performance parameters.

Table 5.7: Experimental data on the effect of various conc. of drilling fluids on the performance parameters

Sr (1)	Poly and con. (2)	Depth (mm) (3)	For 3 min duration (By Video) Time (min) (4)	Depth (cm) (5)	Energy (kWh) (6)	For 5 cm depth of hole (By Video) Depth (mm) (7)	Time (min) (8)	Energy (kWh) (9)	Bit Temp (C°) (10)	Atm. Temp (C°) (11)	Vib. RMS x,y,z (m/s²) (12)	Vib. VTV (m/s²) (13)	Total Energy (kWh) (14)	Energy in Drilling (kWh) (15)	Vol. of hole (mm³) (16)	SEC 10^{-5} (kWh/mm³) (17)	ROP (mm/min) (18)	RRR (mm³/min) (19)
1	Water	50 mm -	0	1	0.468	10	0.10	0.468	42.4	29.8	0.1017	0.135	15.41	3.27	8517.25	38.39	8.15	1388.68
			1	2.4	3.018	20	0.50	2.156			0.0700							
			2	3.5	5.759	30	1.39	4.292			0.0550							
			3	4.2	8.422	40	2.46	7.359			—							
			4	4.7	10.671	50	4.47	12.072			—							
			5	5.2	12.998	60	6.18	15.882			—							
			6	5.9	15.528													

5.7.2.1 Effect on ROP

It was observed that the highest ROP achieved under the effect of different concentrations of individual drilling additives are CMC 70 ppm, GG 50 ppm, PAM 90 ppm, PAMPS 70 ppm, St-g-PAM 10 ppm, St-g-PAMPS 70 ppm, AP-g-PAM 10 ppm, Hy-St-g-PAM 90 ppm, and Hy-AP-g-PAM 90 ppm and their comparative study has been shown in Fig. 5.18.

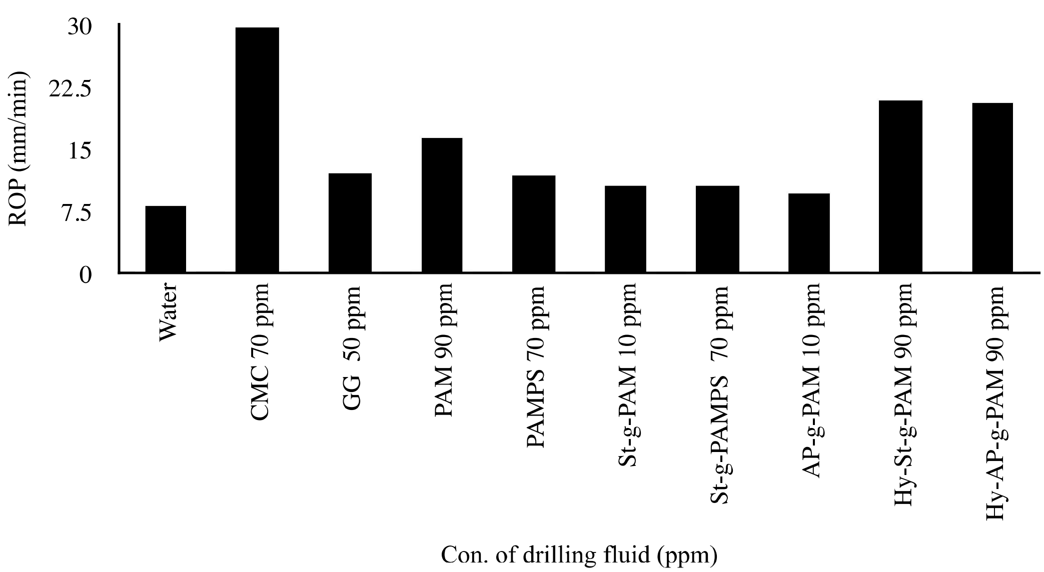

Fig. 5.18: Effect of different drilling fluids on ROP

And among all the drilling fluids, CMC 70 ppm helped in achieving the maximum ROP with 260.78% increment compared to the tap water as drilling fluid. The sequence of best ROP is :CMC > Hy-St-g-PAM > Hy-AP-g-PAM > PAM > GG > PAMPS > St-g-PAM > ST-g-PAMPS > AP-g-PAM (as shown in Fig. 5.18).

5.7.2.2 Effect on Energy Consumption in Drilling

From the experimental data, it was noticed that the lowest energy required in drilling operation, under the effect of different concentrations of individual drilling additives are CMC 10 ppm, GG 50 ppm, PAM 110 ppm, PAMPS 110 ppm, St-g-PAM 10 ppm, St-g-PAMPS 90 ppm, AP-g-PAM 10 ppm, Hy-St-g-PAM 70 ppm, and Hy-AP-g-PAM 110 ppm and their comparative study has been shown in Fig. 5.19. Among all the drilling fluids, minimum energy consumption was for CMC 10 ppm with 91.75% decrement compared to the tap water. The sequence of best energy consumption (as discussed above) is: CMC< Hy-St-g-PAM< PAMPS<Hy-AP-g-PAM< PAM< St-g-PAMPS<GG< AP-g-PAM <St-g-PAM (as shown in Fig. 5.19).

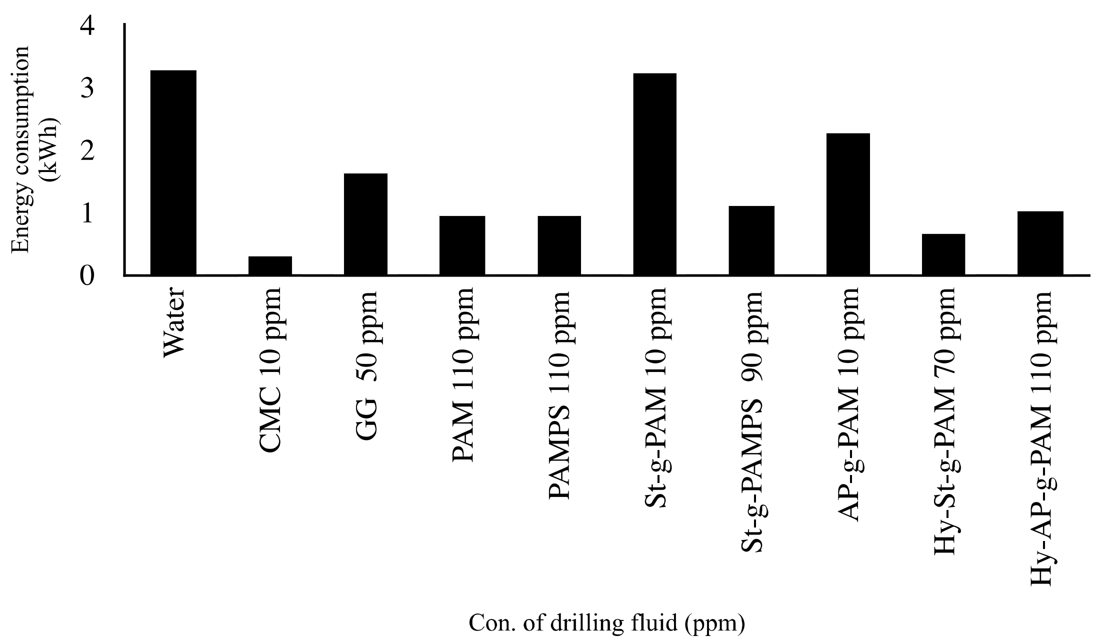

Fig. 5.19: Effect of different drilling fluids on energy consumption in drilling

5.7.2.3 Effect on Specific Energy consumption (SEC)

From the experimental results, SEC values were calculated, and graphically presented for all the drilling fluids. It was noticed that the lowest specific energy consumption was achieved for CMC 10 ppm, GG 50 ppm, PAM 110 ppm, PAMPS 110 ppm, St-g-PAM 10 ppm, St-g-PAMPS 90 ppm, AP-g-PAM 10 ppm, Hy-St-g-PAM 70 ppm, and Hy-AP-g-PAM 70 ppm, and their comparative study has been shown in Fig. 5.20. Among all the drilling fluids, with CMC 10 ppm, the SEC was minimum with 90.91% decrement compared to the tap water as drilling fluid. The sequence of best SEC (as discussed above) is:CMC<Hy-St-g-PAM<PAM<PAMPS<Hy-AP-g-PAM<ST-g-PAMPS<GG<AP-g-PAM<St-g-PAM (as shown in Fig. 5.20).

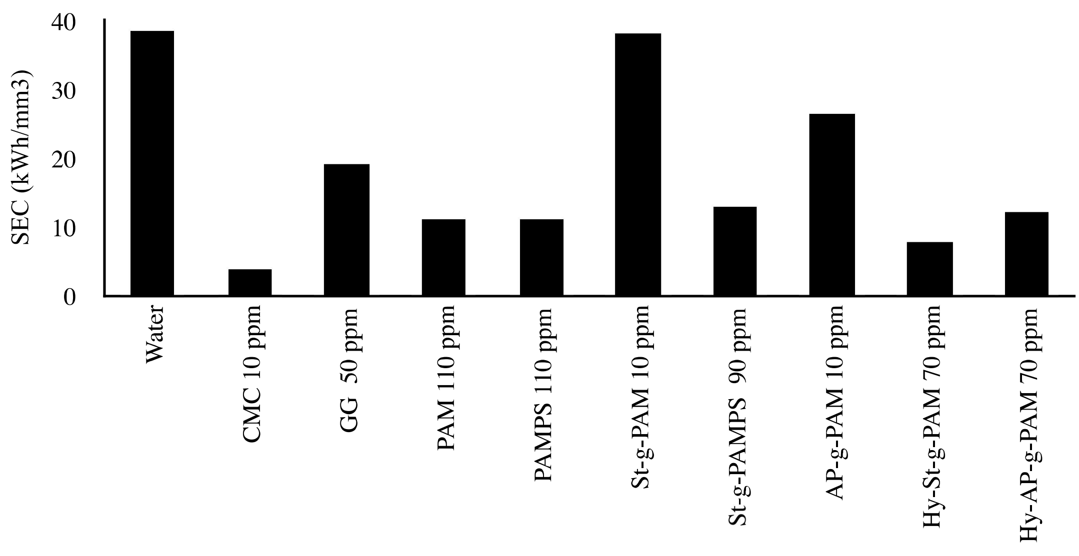

Fig. 5.20: Effect of different drilling fluids on Specific energy consumption (SEC)

5.7.2.4 Effect on Rock Removal Rate (RRR)

It was observed that the highest RRR in drilling, under the effect of different concentrations of individual drilling additives were achieved with CMC 70 ppm, GG 50 ppm, PAM 90 ppm, PAMPS 70 ppm, St-g-PAM 10 ppm, St-g-PAMPS 70 ppm, AP-g-PAM

10 ppm, Hy-St-g-PAM 90 ppm, and Hy-AP-g-PAM 90 ppm. Their comparative study has been shown in Fig. 5.21. RRR was maximum for CMC 70 ppm with 260.78% increment compared to the tap water. The sequence of best RRR (as discussed above) is: CMC>Hy-St-g-PAM>Hy-AP-g-PAM>PAM>GG>PAMPS>St-g-PAM>ST-g-PAMPS>AP-g-PAM (as shown in Fig. 5.21).

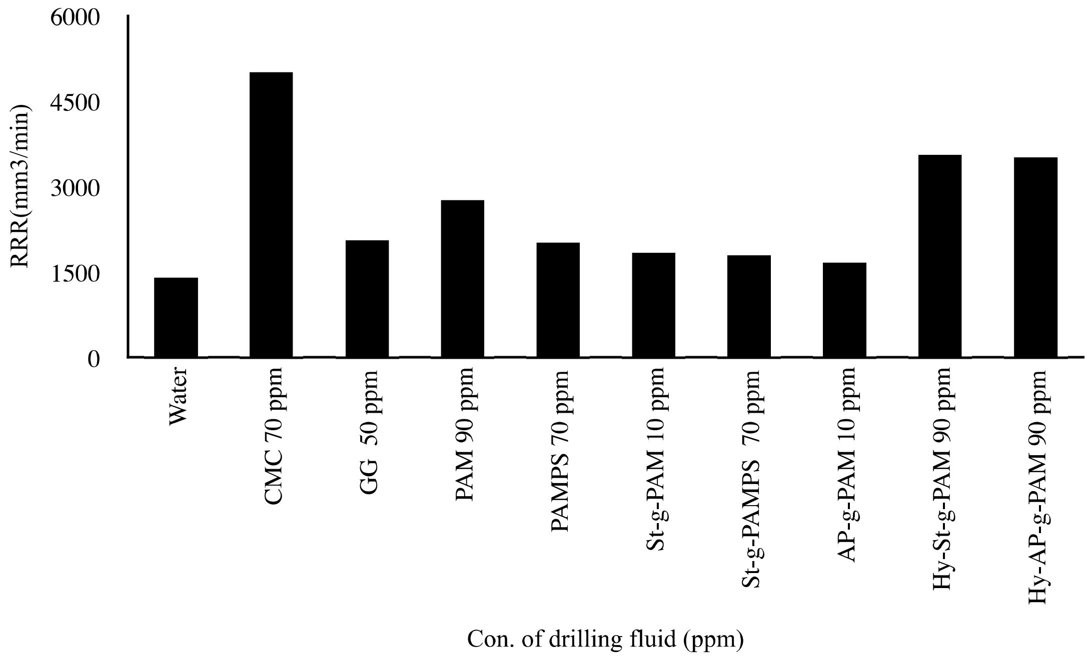

Fig. 5.21: Effect of different drilling fluids on RRR(mm3/min)

5.7.2.5 Effect on Bit Temperature

After drilling the desired depth, temperature of the cutting tip of the bit was measured for all the drilling fluids, and the same has been presented graphically in Fig. 5.22. It was noticed that the lowest bit temperature, under the effect of different concentrations of individual drilling additives were, CMC 110 ppm, GG 30 ppm, PAM 70 ppm, PAMPS 70 ppm, St-g-PAM 110 ppm, St-g-PAMPS 30 ppm, AP-g-PAM 30 ppm, Hy-St-g-PAM 50 ppm, and Hy-AP-g-PAM 110 ppm (as shown in Fig. 5.22). Among all the drilling fluids, with CMC110 ppm, the bit temperature was minimum with 22.40% decrement compare to the tap water as drilling fluid. The sequence of best bit temp. (as discussed above) was

CMC<Hy-AP-g-PAM<Hy-St-g-PAM<ST-g-PAMPS<PAM<AP-g-PAM<GG<St-g-PAM<PAMPS (as shown in Fig. 5.22).

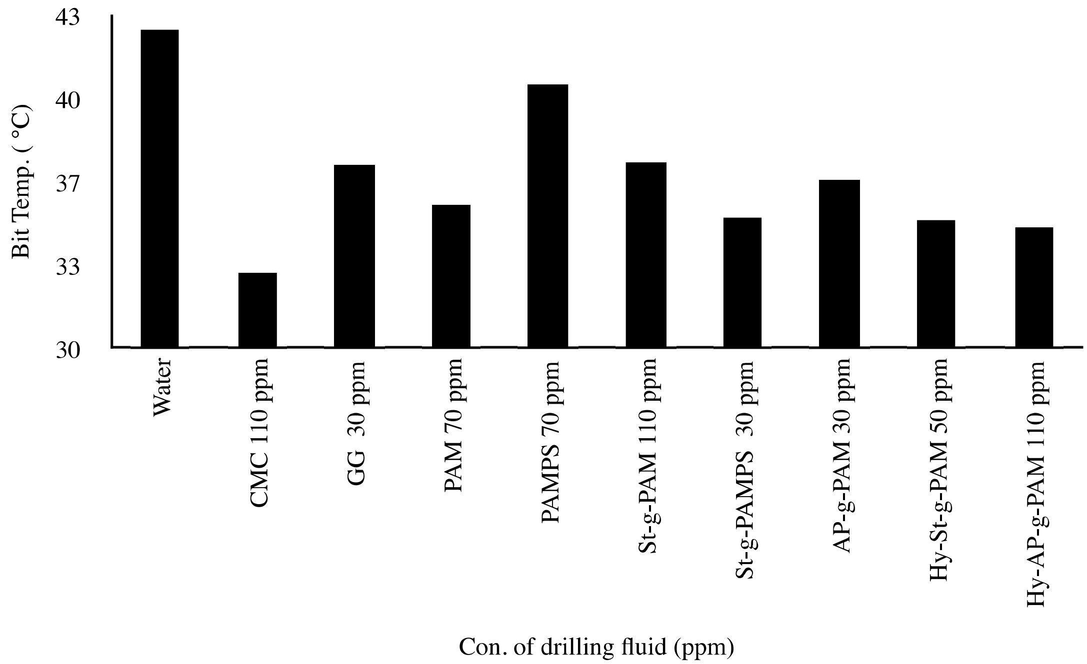

Fig. 5.22: Effect of different drilling fluids on bit temp.

5.7.2.6 Effect on Drill Spindle Vibration

It was observed that the lowest bit temperature after drilling predefined depth, under the effect of different concentrations of individual drilling additives were achieved in, CMC 90 ppm, GG 110 ppm, PAM 110 ppm, PAMPS 110 ppm, St-g-PAM 30 ppm, St-g-PAMPS 90 ppm, AP-g-PAM 50 ppm, Hy-St-g-PAM 30 ppm, and Hy-AP-g-PAM 30 ppm and their comparative study has been shown in Fig. 5.23. And among all the drilling fluids, Hy-St-g-PAM 30 ppm, was found most efficient in reducing bit temperature with 53.48 % decrement compare to the tap water as drilling fluid.. The sequence of best drill spindle vibration (as discussed above) was Hy-St-g-PAM<St-g-PAM.<Hy-AP-g-PAM<AP-g-PAM<PAMPS<CMC<PAM<ST-g-PAMPS<GG (as shown in Fig. 5.23).

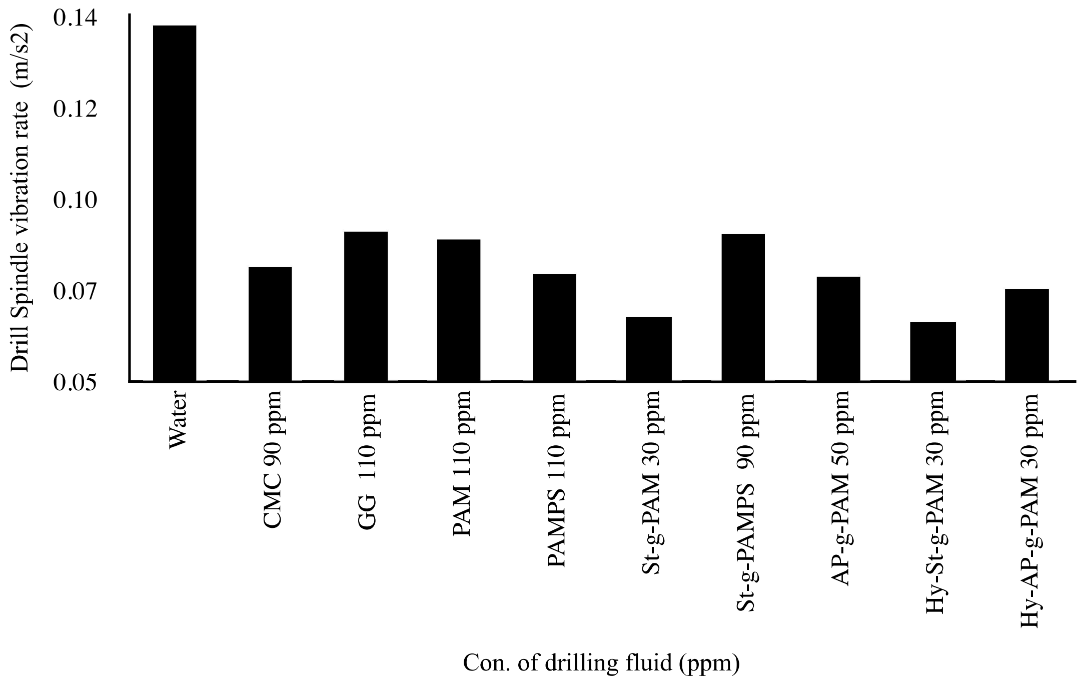

Fig. 5.23: Effect of different drilling fluids on drill spindle vibration

Explanation of the above results

As the discussion on the effect of drilling fluid additives (polymer, grafted and hydrolysed) on the basis of overall drilling performance i.e. 'most optimum performance, while considering the effect on all the drilling parameters together', the CMC, GG, PAM, PAMPS, and Hy St-g-PAM are having more shear viscosity (as shown in Table 4.1), and they were supposed to show better results. But, PAM is having nitrogen as a special element, whereas PAMPS is having both nitrogen and sulphur as special elements, which make them more prone to break under external forces like heat and pressure. PAM and PAMPS are non-polysaccharide (synthetic polymer), whereas CMC, GG, St and AP are polysaccharide (natural polymer). Among these polysaccharide (natural polymer), CMC belongs to liner structure and others are branched structures. Liner structure of CMC leads to layered arrangements of polymer chains, which shows the higher stability. Furthermore, CMC has beta glycosidic linkage, which provides more resistance to break under forces.

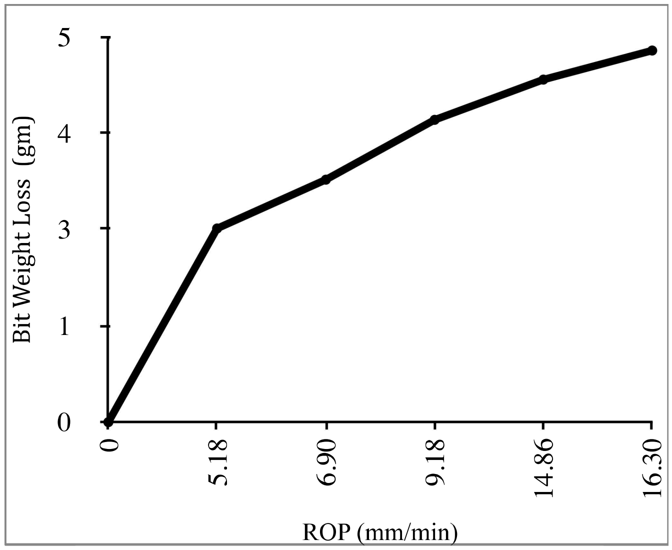

Fig. 5.24: Effect of ROP on Bit Wearing

The amylopectin (AP) is a branched polymer, which leads to the reduction in shear viscosity, and it is true for its co-polymers too. Starch consists of both amylose – a linear structure, and amylopectin – a branched structre. Thus, presence of amylose, make them more stable compared to the amylopectin grafted co-polymers. Grafting and hydrolysis of polymers may lead to the dense branching of a compound, which increases the resistance toward deformation by external forces and, thereby, increases the stability. And, the linearity of a compound also plays vital role in performing as a drilling fluid. Hence, the best drilling performance was achieved with CMC and Hy-st-g-PAM as drilling fluid additives.

5.7.2.7 Effect on Bit Wearing

In this experimental study, the effect of five different ROPs on bit wearing was measured initially by keeping the other parameters constant – namely rock type (sandstone), bit type & size (impregnated diamond core bit of 19/12 mm dia.), load on bit (75.32 N), flushing media (tap water), rate of fluid flushing (31.5 l/h), and depth of the hole (500 mm). The results are presented in Table 5.8 and Fig. 5.24. The amount of rock encountered with the bit depends on the depth of hole achieved by drilling, and the rate of rock encountered depends on the RPM of the bit. In other words, the rate of penetration, will be directly proportional to the rate of rock removal from the hole. So, the bit—rock interaction may cause bit wearing due to the friction and the heat generation in rock cutting process [Bhatnagar et al. 2010].

Table 5.8. Bit Weight loss at different ROP (at 5 kg Load on Bit and Tap Water as Drilling Fluid)

S. No.	Bit Rotation Speed (RPM)	ROP (mm/min)	Drilled Depth (mm)	Bit weight Loss (g)
1	450	5.18	500	2.512
2	600	6.90	500	3.145
3	750	9.18	500	3.921
4	1350	14.86	500	4.443
5	1500	16.30	500	4.820

From the results shown in Fig. 5.24, it can be inferred that bit wearing has increased with the ROP and bit rotational speed. This finding corroborates the results of Bhatnagar et al. (2010) and Miller et al.(1990). As guided by the findings as shown in Fig. 5.24, to identify the role of 10 ppm concentration of 3 different polymeric fluid additives (namely CMC, PAM, and guar gum) and water as drilling fluid on bit wearing, initially a constant ROP was achieved by varying Load on bit and bit rotation speed (as shown in Table 5.9).

Table 5.9: Bit Weight Loss with Various Drilling Fluids (10 ppm)

S. No.	Drilling Fluid Additive (10 ppm)	Load on Bit (N)	Bit Rotation Speed (RPM)	ROP (mm/min)	Depth of Drilling (mm)	Bit weight loss (gm)
1	Water	75.32	1350	14.86	500	4.443
2	CMC	75.32	675	14.80	500	1.332
3	GG	75.32	525	14.73	500	1.947
4	PAM	75.32	750	14.90	500	2.561

Afterward, the respective effect of aforesaid drilling fluids on bit wear was measured and results have been presented in Table 5.9 and Figure 5.25.The bit wearing was considered as one of the performance parameters. In other words, lesser the bit weight loss, better is the drilling performance. Tap water has been used as a successful coolant and flushing medium in previous studies (Miller et al. 1991). From the results shown in Table 5.9 and Figure 5.25, it could be concluded that, the aqueous solution of 10 ppm concentration of all polymeric drilling fluid additives i.e. CMC, guar gum and PAM have shown less bit wearing, and hence, better performance compared to tap water alone. It may be due to the high lubricating property of polymeric drilling fluids, which causes the reduction in frictional force at the bit-rock interface.

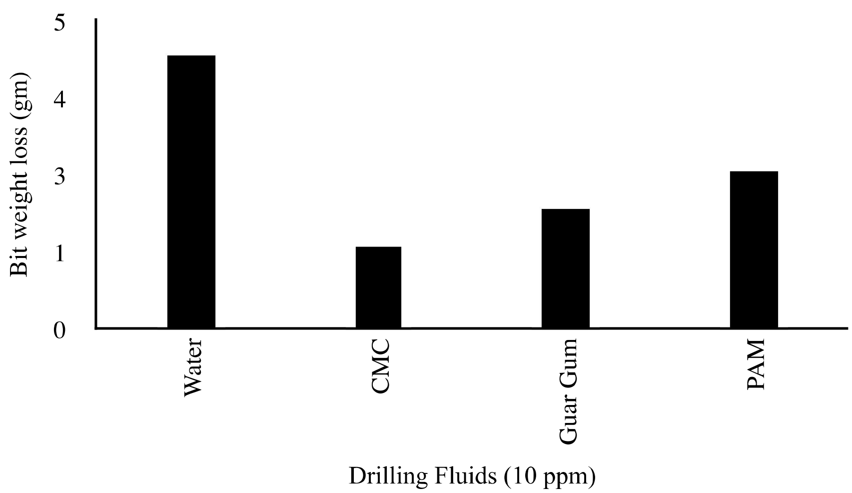

Fig. 5.25: Effect of Various Drilling Fluids on Bit Wearing.

Explanation of the above results

The bit cooling effect through heat dissipation from bit surface by the flow of drilling fluid is also an important factor. Furthermore, the viscosity of polymeric fluids is higher than that of water. So, the fluid with high viscosity can produce greater force at the surfaces of micro-cracks. As a result, it may enhance the rock-breaking efficiency of the drill bit, and reduce the bit wearing compared to tap water. Considerable differences have been observed in the performance of the drilling fluids used in this study. In case of polyacrylamide (PAM) as drilling fluid, bit wearing is maximum when compared with the other two additives. On the other hand, due to the minimum bit wearing with CMC, the best drilling performance was recorded as shown in Figure 5.25. The aqueous solutions of the polymeric drilling fluid additives, used in this study, are highly viscous and also act as lubricant. During drilling process, the flushing fluid generates mechanical shear force exerted by the torsional force in the annular space due to the rotation of down-the-hole assembly (i.e. drill rod, hammer, and bit). So, in the rotary drilling process shear viscosity would be more effective. The shear viscosity of CMC is greater than that of the other two fluid additives used in the study (Ramos et al. 2020, Xia et al. 2020).

Using the polymeric fluids, the friction at the bit-sidewall interface can be controlled, and it is expected to help in reducing the bit wearing. With the increasing viscosity of drilling fluids, the lubrication property would also be improved by the additives used in this study. The high viscous fluid is capable of exerting comparatively high pressure on the inner surface of cracks. This is responsible for the most effective expansion of pre-existing micro-cracks leading to the weakening of rock surface. It would be more convenient for the bit to drill weak rock surface, with minimum wear and tear. This phenomenon of high viscous fluids may enhance the drilling efficiency, and reduce the bit wearing compared to the low viscous ones. Thus, it can be inferred that the reduction in bit wearing is most effective, up to 70.02 % with CMC-based drilling fluid, compared to the tap water as base drilling fluid under the working conditions prevailing in this study.

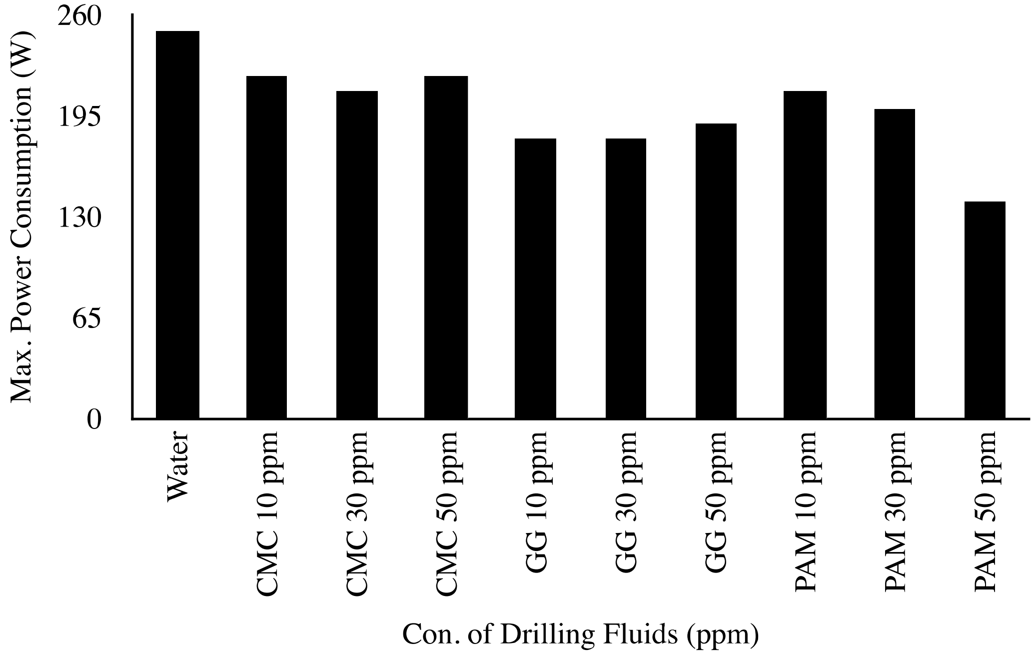

Fig. 5.26: Power Consumption at 750 RPM at 75.32 N load

5.7.2.8 Effect on Peak Power Consumption

The data for power consumption for all the combinations of the operating parameters are summarised in Table 5.10. The minimum power consumption values (column 3 of Table 5.10) were shown by the wattmeter at the initial bit—rock interaction. A graphical representation of the results is given in Fig. 5.26. At this surficial interaction, the bit has minimum or negligible resistance on its side wall. Also, there was no penetration in the rock or no generation of drill cuttings at the stage of initial interaction. In the absence of drill cuttings, the primry role of drilling fluid (i.e. hole cleaning) was not needed to be accomplished. So, the minimum power consumption value has no effect of drilling fluid and also it was constant for individual combinations of bit rotation speed and load on the bit. From the result of the study, a constant increment was noticed in minimum and in maximum power consumption - both with the bit rotation speed and load on bit as shown

Table 5.10 and Fig. 5.26. It may be due to the increase in torque requirement with rotation speed as well as the load on the bit (Rao et al. 2010).

Table 510: Experimental Data for Power Consumption

(1) Bit Rotational speed (RPM)	(2) Load on Bit (N)	(3) Min Power consump^{n} (w)	(4) Maximum Power consumption (W) for									
			Tap Water	CMC (ppm)			GG (ppm)			PAM (ppm)		
				10	30	50	10	30	50	10	30	50
150	36.09	50	80	80	70	70	60	60	60	70	60	60
	55.7	60	90	90	80	80	80	70	70	80	70	70
	75.32	70	120	110	100	90	110	90	80	90	80	80
300	36.09	60	90	90	80	70	80	70	70	70	60	60
	55.7	70	120	110	90	90	90	80	80	80	80	70
	75.32	80	140	130	110	110	110	100	100	100	90	90
450	36.09	70	100	90	80	80	80	80	80	80	80	80
	55.7	80	140	120	110	100	100	90	90	100	90	90
	75.32	90	160	150	130	130	120	120	100	130	130	100
600	36.09	80	110	110	90	90	100	90	90	90	90	100
	55.7	90	160	150	120	130	120	120	110	120	110	110
	75.32	100	190	170	160	170	150	150	170	160	160	110
750	36.09	90	150	120	120	110	100	100	100	110	110	100
	55.7	100	200	170	160	160	130	140	130	160	150	110
	75.32	120	250	220	210	220	180	180	190	210	200	140

Again, a decrement in power consumption was observed while drilling with all polymer additives compared to tap water at each combination of RPM and load. It is because polymeric additive fluids are more viscous than water (viscosity 2021), (as shown in Table 5.10), and viscosity is directly proportional to its lubrication properties, which causes a reduction in frictional coefficient at bit—rock interface (Gwidon et al. 2005). This reduction in frictional coefficient may ease the rotation of the drill string in the annular space of the hole, and thereby, reduce the power input requirement to overcome drag between the drill string and the hole wall. The maximum power consumption has reduced with the increment in concentration of drilling fluid additives from 10 ppm to 30 ppm, for all combinations of machine parameters. This increment in ppm concentration may cause the increase in viscosity and reduction in power consumption. But, with further increment in concentration (upto 50 ppm) for CMC and guar gum based drilling fluids, the maximum power consumption has increased. It may be due to the thickening of drilling mud (i.e. fluid returning from the hole bottom taking away the drill cuttings) with high viscous fluid. This thickening of mud may result in the high power consumption to overcome the increased torque development. On the other hand, with PAM additives, at low concentration (i.e. 10 ppm to 30 ppm), no considerable improvement in power consumption is observed. But whereas with PAM 50 ppm concentration, the peak power consumption in drilling, dropped maximum.

The combination of 750 RPM bit rotational speed and 75.32 N load on the bit has shown maximum power consumption for all drilling fluids, due to increase in torque requirements in drilling. So, it was considered most convenient for graphical representation, to understand the effect of different drilling fluids (as shown in Figure 5.26). While observing the effect of 50 ppm concentration of all the fluids, the maximum power consumption was decreased with the increment in dynamic viscosity (as given in Table 5.10). The lowest power consumption was identified in drilling with 50 ppm concentration of PAM additive (Table 5.10 and Figure 5.26), with 44 % decrement as compared to tap water alone. Among the three different polymeric fluids, PAM has the highest shear stability. This is because CMC and GG are polysaccharide in nature which leads to break down of glycosidic linkages under higher shear rate.

5.8 Selection of the Best Performing Drilling Fluid

For all the fluid additives used in this study, best ppm concentration has been shown in table 5.11 individually, which helps to improve the drilling performance. Whereas, the order of best drilling fluid, based on their performance with respect to various drilling parameters is given in table 5.12. The list of best fluid for individual drilling parameter is shown in table 5.13.

For the selection of the best drilling fluid additive among all alternative (used in this experiment) to improvise overall performance, based on various criteria (output parameters) namely ROP, energy consumption, SEC, vibration, RRR, and bit temperature, Weighted Sum Model (WSM) of Multi-Criteria Decision Making (MCDM) method has been used with the help of table 5.12. As per Yang (2014), the weighted sum model is very efficient, simple, and universally accepted for decision-making for a vast variety of areas like as school selection for fund allocation [Handoko 2017], supplier selection for industries [Dwivedi and Dwivedi 2018], selecting the optimal material for engineering product design [Godwin 2018], total emissivity and absorptivity may be represented by the sum of a grey gas emissivity weighted with a temperature-dependent factor [Smith et al. 1982].

To identify the best drilling fluid, based on different performance parameters, a normalized decision matrix has been prepared by dividing the lowest value (column-wise) form each entry in the column (from Table 5.12) and presented in table 5.14.

Table 5.11: Best performing ppm con. for individual fluid additive

Sr.	Parameters → / Poly Add. ↓	1		2		3		4		5		6	
		ppm	**ROP** (mm/min)	ppm	**Energy (kWh)**	ppm	**SEC (kWh /mm³)**	ppm	**RRR (mm³/ min)**	ppm	**Bit Temp (C°)**	ppm	**Vibr.** (m/s²)
1	CMC	70	29.41	10	0.3	10	3.49	70	5010.15	110	32.9	90	0.0779
2	GG	50	12.05	50	1.62	50	10.03	50	2052.35	30	37.1	110	0.0868
3	PAM	90	16.22	110	0.92	110	10.79	90	2762.35	70	34.6	110	0.0847
4	PAMPS	70	11.76	110	0.64	110	7.56	70	2004.06	70	40.3	110	0.0759
5	St-g-PAM	10	10.6	10	3.22	10	37.85	10	1805.78	110	37.2	30	0.656
6	St-g-PAMPS	110	9.71	90	1.08	90	12.66	110	1653.71	30	35.1	90	0.086
7	AP-g-PAM	10	9.68	10	2.25	10	26.46	10	1648.5	30	36.5	50	0.0754
8	Hy-St-g-PAM	90	20.83	90	0.27	90	3.16	90	3548.85	50	35.0	30	0.064
9	Hy-AP-g-PAM	90	20.55	70	0.66	70	7.79	90	3500.24	110	34.7	30	0.0726

Table 5.12: Sequence of best drilling fluid based on their performance

Perform -ance order	**ROP (mm/min)**	**Energy (kWh)**	**SEC (kWh/ mm³)**	**RRR (mm³/min)**	**Bit Temp (C°)**	**Vibration (m/s²)**
1	CMC 70 ppm	Hy-St-g-PAM 90 ppm	Hy-St-g-PAM 90 ppm	CMC 70 ppm	CMC 110 ppm	Hy-St-g-PAM 30 ppm
2	Hy-St-g-PAM 90 ppm	CMC10 ppm	CMC 10	Hy-St-g-PAM 90 ppm	PAM 70 ppm	Hy-AP-g-PAM 30 ppm
3	Hy-AP-g-PAM 90 ppm	PAMPS 110 ppm	PAMPS 110	Hy-AP-g-PAM 90 ppm	Hy-AP-g-PAM 110 ppm	AP-g-PAM 50 ppm
4	PAM 90 ppm	Hy-AP-g-PAM 70 ppm	Hy-AP-g-PAM 70	PAM 90 ppm	Hy-St-g-PAM 50 ppm	PAMPS 110 ppm
5	GG 50 ppm	PAM 110 ppm	GG 50	GG 50 ppm	St-g-PAMPS 30 ppm	CMC 90 ppm
6	PAMPS 70 ppm	ST-g-PAMPS 90 ppm	PAM 110	PAMPS 70 ppm	AP-g-PAM 30 ppm	PAM 110 ppm
7	St-g-PAM 10 ppm	GG 50 ppm	ST-g-PAMPS 90	St-g-PAM 10 ppm	GG 30 ppm	ST-g-PAMPS 90 ppm
8	ST-g-PAMPS 110 ppm	AP-g-PAM 10 ppm	AP-g-PAM 10	ST-g-PAMPS 110 ppm	St-g-PAM 110 ppm	GG 110 ppm
9	AP-g-PAM 10 ppm	St-g-PAM10 ppm	St-g-PAM 10	AP-g-PAM 10 ppm	PAMPS 70 ppm	St-g-PAM 30 ppm

During this experimental study, it is observed that variation of each and every parameter has some impact on the result i.e. drilling efficiency. For the sake of simplicity, in this study all the parameters have been given equal weightage for WSM (as presented in Table

5.15), and multiplied with each normalized cell value in the matrix, to prepare weighted normalized matrix as presented in Table 5.16.

Table 5.13: Best fluid for individual drilling parameter

Sr.	Drilling Parameter	Best Performing Drilling Fluid Additive with con.
1	ROP (mm/min)	CMC 70 ppm
2	Energy (kWh)	Hy-St-g-PAM 90 ppm
3	SEC (kWh/mm^3)	Hy-St-g-PAM 90 ppm
4	Vibration (m/s^2)	Hy-St-g-PAM 30 ppm
5	RRR (mm^3/min)	CMC 70 ppm,
6	Bit temp (C^o)	CMC110 ppm
7	*Bit wear	CMC 10 ppm
8	*Peak Power consumption	PAM 50 ppm
* Limited additives have been tested for this parameter.		

Table 5.14: Normalised Decision matrix (for WSM method)

Sr.	Poly Add.	ROP (mm/min)	Energy (kWh)	SEC (kWh/ mm^3)	RRR (mm^3/min)	Bit Temp (C^o)	Vibr. (m/s^2)
1	CMC	29.41/29.41	0.27/0.3	3.16/3.49	5010.15/5010.15	32.9/32.9	0.064/0.0779
2	GG	12.05/29.41	0.27/1.62	3.16/10.03	2052.35/5010.15	32.9/37.1	0.064/0.0868
3	PAM	16.22/29.41	0.27/0.92	3.16/10.79	2762.35/5010.15	32.9/34.6	0.064/0.0847
4	PAMPS	11.76/29.41	0.27/0.64	3.16/7.56	2004.06/5010.15	32.9/40.3	0.064/0.0759
5	St-g-PAM	10.6/29.41	0.27/3.22	3.16/37.85	1805.78/5010.15	32.9/37.2	0.064/0.656
6	St-g-PAMPS	9.71/29.41	0.27/1.08	3.16/12.66	1653.71/5010.15	32.9/35.1	0.064/0.086
7	Amy-g-PAM	9.68/29.41	0.27/2.25	3.16/26.46	1648.5/5010.15	32.9/36.5	0.064/0.0754
8	Hy-St-g-PAM	20.83/29.41	0.27/0.27	3.16/3.16	3548.85/5010.15	32.9/35.0	0.064/0.064
9	Hy-Amy-g-PAM	20.55/29.41	0.27/0.66	3.16/7.79	3500.24/5010.15	32.9/34.7	0.064/0.0726

Thereafter, for the deciding performance score of individual drilling fluid, row wise sum up of the values in each cell has been done to get preference score, and each fluid have a preference score based on which, they have been ranked. The higher value of cumulative sum represents higher rank (or preference). As per the performance score and rank (given in table 5.16), based on weightage assigned to each parameter (equal weightage), to improve the overall drilling performance, as best drilling fluid additive Hy-St-g-PAM 90 ppm (rank 1), may be chosen for working conditions used in this experiment. In the case of unavailability of Hy-St-g-PAM, next best (rank 2) CMC based additives can be utilised as drilling fluid additive, and so on.

Table 5.15: Weightage allotment to all parameters (for WSM method)

Sr.	Weightage	**16.66**	**16.66**	**16.66**	**16.66**	**16.66**	**16.66**
	Poly Add.	**ROP** (mm/min)	**Energy (kWh)**	**SEC (kWh/ mm^3)**	**RRR (mm^3/ min)**	**Bit Temp (C^o)**	**Vibr.** (m/s^2)
1	CMC	1	.9	.905	1	1	.821
2	GG	0.409	.166	.315	.409	.886	.737
3	PAM	0.551	.293	.292	.551	.950	.755
4	PAMPS	0.399	.421	0.417	04	.816	.843
5	St-g-PAM	.360	.083	0.083	.360	.884	.097
6	St-g-PAMPS	.330	.25	.249	.330	.937	.744
7	Amy-g-PAM	0.329	0.12	.119	.329	.901	.848
8	Hy-St-g-PAM	.708	1	1	.708	.94	1
9	Hy-Amy-g-PAM	.698	.409	.405	.698	.948	.881

Table 5.16:Weighted normalized decision matrix, performance score and rank of drilling fluid additives (with WSM method)

Sr	**Poly Additives**	**ROP** (mm/min)	**Energy (kWh)**	**SEC (kWh/ mm^3)**	**RRR (mm^3/ min)**	**Bit Temp (C^o)**	**Vibr.** (m/s^2)	**Performa-nce score**	**Rank**
	Weightage	**16.66%**	**16.66%**	**16.66%**	**16.66%**	**16.66%**	**16.66%**		
	Categorization	Beneficial	Non beneficial	Non beneficial	Beneficial	Non beneficial	Non beneficial		
1	CMC	.166	.9	.905	1	1	.821	4.792	2
2	GG	0.409	.166	.315	.409	.886	.737	2.922	6
3	PAM	0.551	.293	.292	.551	.950	.755	3.392	4
4	PAMPS	0.399	.421	0.417	0.4	.816	.843	3.296	5
5	St-g-PAM	.360	.083	0.083	.360	.884	.097	1.867	9
6	St-g-PAMPS	.330	.25	.249	.330	.937	.744	2.84	7
7	AP-g-PAM	0.329	0.12	.119	.329	.901	.848	2.646	8
8	Hy-St-g-PAM	.708	1	1	.708	.94	1	5.356	1
9	Hy-AP-g-PAM	.698	.409	.405	.698	.948	.881	4.039	3